Potential Vorticity in Hurricane Gloria

LLOYD J. SHAPIRO AND JAMES L. FRANKLIN

Hurricane Research Division, AOML/NOAA, Miami, Florida

(Manuscript received 2 March 1994, in final form 1 July 1994)

ABSTRACT

Potential vorticity (PV) analyses for Hurricane Gloria of 1985 are derived from nested objective wind analyses of Omega dropwindsonde and airborne Doppler radar data. The analyses resolve eyewall-scale features in the inner vortex core and embed analyses of these features within the larger-scale environment. Since three-dimensional geopotential height fields required for evaluation of PV are not available in the core, they are derived using the balance equation. In the process of deriving the heights, the degree of gradient balance is evaluated. The 500-mb tangential winds in the core, averaged azimuthally on the four cardinal points, are close to gradient balance outside the radius of maximum wind.

The resulting depiction of PV is the first presented for a real hurricane. Due to data deficiencies immediately outside the Doppler region, as well as inside the eye, smoothing of the wind data using a filter with a minimum 25-km spatial scale is required to derive a balanced geopotential height distribution consistent with a statically stable vortex. The large-scale PV distribution evidences asymmetries in the middle and upper troposphere that appear to be associated with Gloria's translation to the northwest. Eyewall-scale PV in the core and PV of the azimuthally averaged vortex are also presented.

1. Introduction

Potential vorticity (PV) has been shown to be a powerful tool for understanding the dynamics of quasi-balanced atmospheric systems. Given three-dimensional fields of wind and geopotential height (or pressure), the PV distribution can be derived. As articulated by Hoskins et al. (1985), the advantages of using PV as a diagnostic quantity are twofold. First, in the absence of diabatic or frictional sources or sinks, PV is conserved following a fluid parcel. Second, if the three-dimensional distribution of PV, a balance condition between the winds and heights, and appropriate boundary conditions are specified, then the wind, pressure, and temperature fields are determined uniquely. The utility of PV analysis in understanding midlatitude cyclogenesis has been demonstrated recently by Davis and Emanuel (1991).

Understanding of tropical cyclone dynamics has also been aided greatly by the use of PV. Thorpe (1985) diagnosed the structure of idealized symmetric vortices for simple PV distributions, while Schubert and Alworth (1987) simulated the evolution of PV in an idealized symmetric model of a tropical cyclone. In a three-layer model, Shapiro (1992) used PV considerations to diagnose and understand the motion and evolution of a hurricane vortex in the presence of vertical shear. Guinn and Schubert (1993a) have modeled the development of hurricane spiral bands with a shallow water system, interpreting the results in terms of PV evolution. Recently, Wu and Emanuel (1995) have used synoptic-scale analyses of real data to diagnose hurricane motion from a PV perspective.

As noted by Guinn and Schubert (1993a), there have been no published depictions of PV in real tropical cyclones. The primary purpose of the present paper is to remedy this situation by deriving PV for Hurricane Gloria of 1985. In a recent study, Franklin et al. (1993; hereafter FLFM) described the kinematic structure of this hurricane, as determined from nested analyses of Omega dropwindsonde (ODW) and airborne Doppler radar data. The data were obtained during a "synoptic-flow" experiment conducted by the Hurricane Research Division (HRD) of the Atlantic Oceanographic and Meteorological Laboratory/National Oceanic and Atmospheric Administration (AOML/NOAA) using two NOAA WP-3D research aircraft. The nested multiscale analyses simultaneously describe Gloria's eyewall and synoptic-scale features. The combination of environmental and vortex core observations is the most comprehensive kinematic dataset ever obtained in a hurricane. Sections 2 and 3 of FLFM thoroughly discuss the data, analysis algorithm, and methodology for the Gloria analyses. Readers unfamiliar with the analyses might wish to refer to the discussion in FLFM or the appendix of the present paper, which gives a brief overview.

One of the reasons for the lack of PV analyses in real hurricanes is the absence of simultaneous high-

Corresponding author address: Dr. Lloyd J. Shapiro, NOAA/AOML/HRD, 4301 Rickenbacker Causeway, Miami, FL 33149.

quality three-dimensional wind and thermodynamic data. FLFM confined their discussion of Gloria to the three-dimensional characteristics of the kinematic fields and their relationship to the hurricane's motion. Wind, vorticity, and kinematically derived vertical motion analyses were presented. The dataset used by FLFM contains a rather limited number of geopotential height observations, however, particularly in the inner core. The synoptic-scale analysis of geopotential height at 500 mb using these data is shown in Fig. 1. As with the wind analyses on this scale (Fig. 5b of FLFM), the vortex represented in the height field is broad and weak. While an ODW drop in the eye gave an observed height of 5268 m at this level (Franklin et al. 1988), the lowest analyzed height near the vortex center in Fig. 1 is approximately 5820 m. The density of height observations, insufficient to resolve the vortex at 500 mb, is even coarser at higher levels.

Since three-dimensional geopotential fields are not available in the hurricane core, they will be derived from the balance equation (e.g., Haltiner and Williams 1980) using appropriate boundary conditions. For a symmetric vortex on an f plane, the balance equation reduces to gradient balance. The equation is derived under the assumption that the divergence and its time tendency are weak. Although large-scale systems are close to nondivergent balance, the degree of balance in the core of a hurricane has been the subject of some controversy (Willoughby 1990b, 1991; Gray 1991). The generalization of the concept of balance to a rapidly rotating vortex such as a hurricane, where divergence may not be weak, is a topic of current investigation (Shapiro and Montgomery 1993). While FLFM did not make a quantitative determination of the degree of gradient or thermal wind balance in Gloria's core, they noted that an inward slope of the radius of maximum wind (RMW) below 550 mb, in the face of strong descent and warming within the eye, suggested a lower-tropospheric mean thermal wind imbalance.

In the process of deriving height fields in section 2a, a quantitative evaluation of gradient wind balance in Hurricane Gloria is made. Data deficiencies make evaluation of temperatures in the hurricane's inner core problematic. In section 2b the smallest spatial scale at which the balance equation can be used, given the data deficiencies, is evaluated. The wind and balanced height fields are then used in section 3 to derive PV distributions for both the inner core and environment of the hurricane. Section 4 discusses the results.

2. Balanced heights

a. Comparison with observed heights

Under the assumption that the wind is nearly nondivergent and the divergence tendency is small, the balance equation can be used to derive the geopotential height distribution from the wind field:

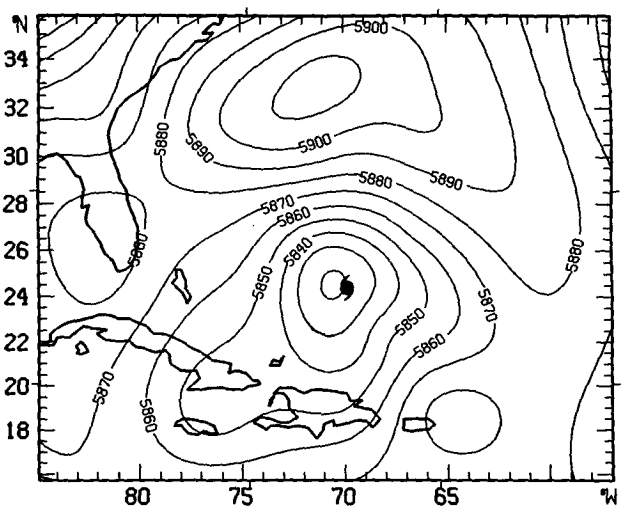

FIG. 1. Synoptic-scale analysis [meshes 6–7; see Table 2 of Franklin et al. (1993) or the appendix of present paper] of 500-mb geopotential height resolving scales greater than 44 km. Contour interval is 10 m. Axis labels are degrees latitude (°N) and longitude (°W).

$$\nabla^2\phi = f_0\zeta - \beta u + 2\left(\frac{\partial u}{\partial x}\frac{\partial v}{\partial y} - \frac{\partial u}{\partial y}\frac{\partial v}{\partial x}\right). \quad (1)$$

Here u and v are the zonal (x) and meridional (y) winds, respectively, and ζ is the relative vorticity. Also, f_0 and β are the Coriolis parameter and its meridional gradient, respectively, at the reference latitude. The geopotential ϕ is operated upon by the horizontal Laplacian ∇^2. If the wind is strictly nondivergent, then (1) is equivalent to Eq. (3-81) of Haltiner and Williams (1980). While synoptic-scale systems in the Tropics approximately satisfy this balance assumption, smaller-scale systems can have substantial divergence, particularly in the presence of convection. The balance equation is inadequate for dealing with intense convective circulations (Fankhauser 1974), such as the inner core of a hurricane vortex. As noted in the appendix, however, the Gloria analyses reveal only the coarser mesoscale motions in the vortex core. At 500 mb the magnitude of the analyzed divergence (Fig. 2a) is generally less than, and in some places much less than, that of the vorticity (Fig. 2b). Consequently, inclusion of the analyzed divergence-associated contributions does not qualitatively change any of the results presented below, which are based on (1).

In order to derive the heights from (1), boundary conditions are required. These are obtained from the analysis shown in Fig. 1 along the indicated boundaries. This region (FLFM's mesh 7, see the appendix) is well sampled by ODWs or rawinsondes. FLFM show the synoptic-scale 500-mb wind field for the same region (their Fig. 5b). Figure 3 shows the derived balanced height field on both the (a) synoptic and (b) vortex core scales. The synoptic-scale balanced heights

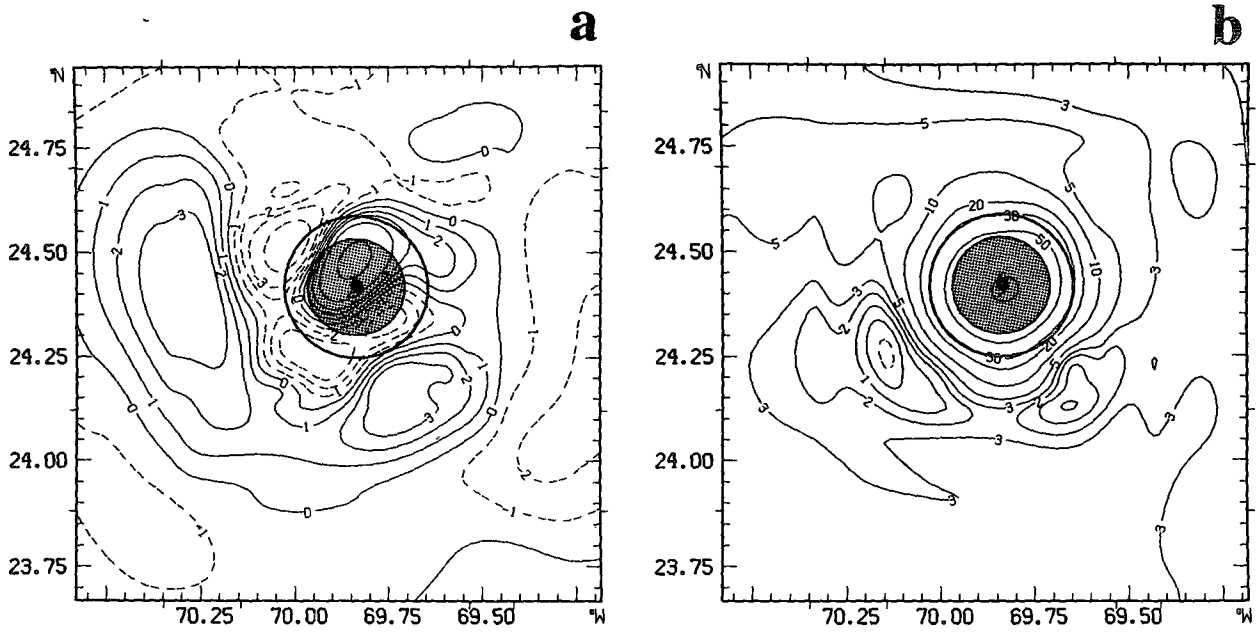

FIG. 2. Analysis of 500-mb (a) divergence and (b) vorticity for Doppler region (meshes 1–3). Contours are 0, ±1, ±2, ±3, ±5, 10, 20, 30, 50, 100 × 10^{-4} s^{-1}. Negative contours are dashed. Stippling delineates data-sparse region within 13 km of vortex center (see the appendix). Circle delineates the 500-mb RMW at 19-km radius.

(Fig. 3a) are close to those observed (Fig. 1) outside of about 300 km of the vortex center.

The balanced heights within the Doppler region (Fig. 3b) are quite symmetric. The difference between the balanced and observed heights in the Doppler region, where wind observations are dense, is shown in Fig. 4. In deriving the analysis of the observed heights, 500-mb rawinsonde and ODW data were supplemented by WP-3D aircraft measurements obtained during the "figure-four" (Doppler) portion of the flight pattern (see section 2a of FLFM). The aircraft heights, observed between 440 and 460 mb, were adjusted hydrostatically to 500 mb using temperature lapse rates determined from nearby ODW soundings. Separate analyses at 450 mb (not shown) confirm that the hydrostatic adjustment has an insignificant effect on the results. The figure-four pattern creates an azimuthally sparse data distribution. Therefore, following FLFM, the data were augmented by concentric rings of interpolated observations, with the heights at each interpolated location determined using a single-pass Barnes (1964) analysis configured in polar coordinates (M. DeMaria 1990, personal communication).

The deviations in Fig. 4 are negative, indicating that the balanced heights are low everywhere within the Doppler region. The largest negative deviations occur inside the eye (indicated by stippling), where Doppler data are nearly absent (see the appendix). At the center the balanced height is 5070 m, about 200 m lower than the observed height of 5268 m from the ODW drop in the eye. The −50- to −70-m deviations at the boundary of the Doppler region are attributable to the overly strong cyclonic circulation of 2–5 m s^{-1} in the 75–275-km radial band noted by FLFM. In the well-sampled region between the RMW and the outer boundary of the Doppler region there remains, however, an outward gradient to the deviations in all directions except to the north. This outward gradient implies that the winds in this region are stronger than required to sustain gradient balance.

Azimuthally averaged observed heights $\bar{z}$, computed about the 500-mb wind center, can be used to derive the symmetric gradient tangential wind $\bar{V}_{gr}$ and thereby quantify the magnitude of the implied supergradient imbalance. In Fig. 5 the azimuthally averaged tangential wind $\bar{V}$ is shown within the Doppler region, together with the difference $\bar{V} - \bar{V}_{gr}$. Here the azimuthal averages are based on only the four cardinal points (at angles 0°, 90°, 180°, and 270°), so as to be very close to the locations of the flight-level measurements.[1] Azimuthal averaging about the balanced-height minimum, instead of the wind center, has a negligible effect on the results. Within the Doppler region but outside the

[1] Outside the RMW, the four-cardinal-point average tangential wind is approximately 1 m s^{-1} weaker than the complete azimuthally averaged wind. The in situ aircraft winds are similarly weaker than the complete azimuthally averaged Doppler winds at flight level (H. Willoughby 1994, personal communication). The implied azimuthal wavenumber 4 asymmetry may be physical or may possibly be analysis induced.

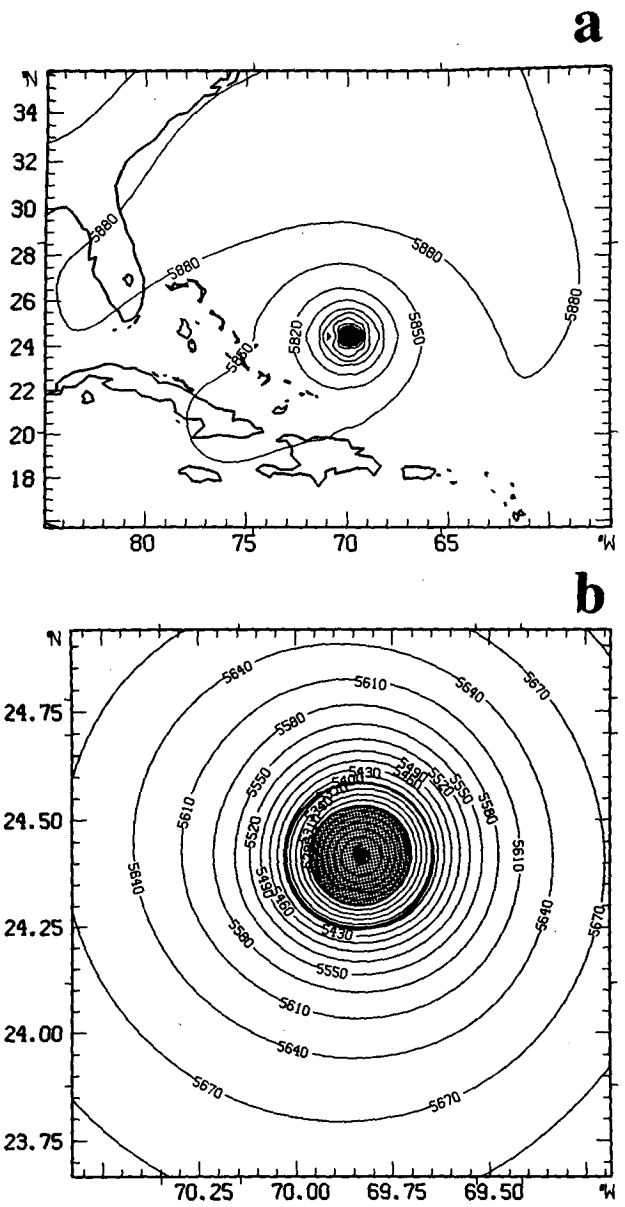

FIG. 3. Balanced heights at 500 mb for (a) synoptic-scale analyses (meshes 6–7; contour interval 30 m) and (b) Doppler region (meshes 1–3; contour interval 10 m). Irregular contours in (a) are due to undersampling of the high-resolution analyses near the vortex center.

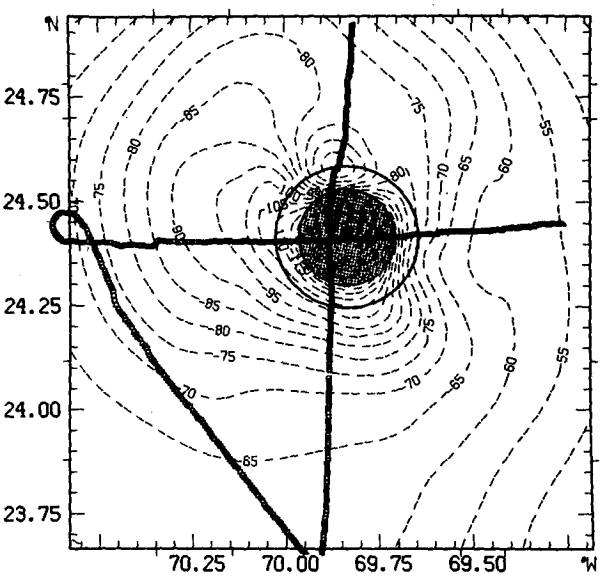

FIG. 4. Difference between balanced and observed 500-mb heights for Doppler region (meshes 1–3). Contour interval is 5 m. Stippling and circle are the same as those in Fig. 2. Locations of height observations are marked by open squares on the figure-four flight track.

RMW, between 19 and 55 km from the vortex center, the average wind imbalance is supergradient ($\bar{V} - \bar{V}_{gr} > 0$) by 1.6 m s^{-1}, with a root-mean-square (rms) difference of 1.8 m s^{-1}.

Unlike $\bar{V}$, the gradient wind $\bar{V}_{gr}$ is derived from radial gradients of filtered analyses of $\bar{z}$. Thus, the spatial scales associated with $\bar{V}$ and $\bar{V}_{gr}$ are not strictly consistent. This scale inconsistency could lead to an apparent imbalance where none exists. As noted by FLFM, the vortex core is filtered somewhat more strongly than is necessary from data considerations alone. In order to evaluate the effect of filtering on the balance, additional 500-mb analyses were made with one-half the filter wavelengths used by FLFM. Deviations of these analyses from the original wind and height observations in the Doppler region were found to be very small and randomly distributed. The imbalance of the resulting winds and heights is also shown in Fig. 5. The differ-

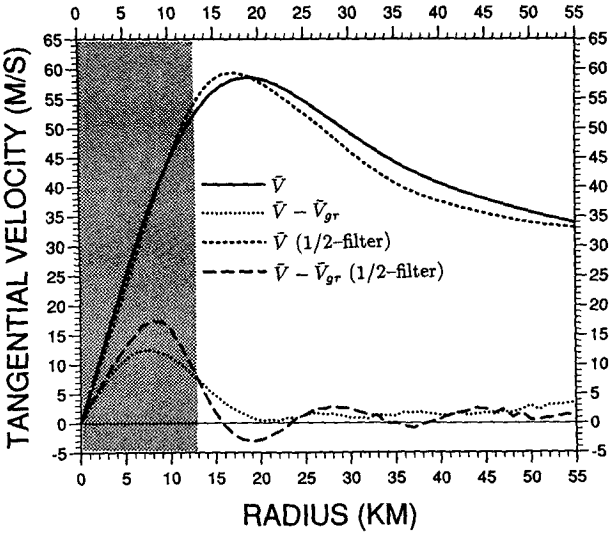

FIG. 5. Azimuthally averaged 500-mb tangential wind $\bar{V}$ and the difference between this wind and the symmetric gradient tangential wind $\bar{V}_{gr}$ based on the four cardinal points. Results for filter wavelengths used by FLFM as well as for filters with one-half these wavelengths are shown. Stippling indicates extent of data-sparse region.

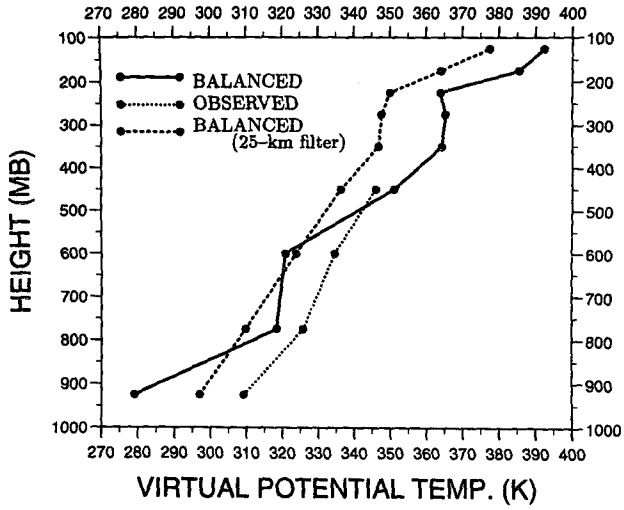

FIG. 6. Virtual potential temperatures at center of Hurricane Gloria using heights from adjacent mandatory levels. Temperatures derived from observed heights, balanced heights, and balanced heights from 25-km-scale analyses are shown.

ence $\bar{V} - \bar{V}_{gr}$ for the half-filtered analyses generally oscillates about that for the full filter. Outside the RMW, imbalances are as large as 3 m s^{-1} in radial bands with scales of about 10 km. The average supergradient imbalance between 19 and 55 km from the vortex center is only 0.8 m s^{-1}, with an rms difference of 1.7 m s^{-1}. Despite the sparse azimuthal sampling in the present study, the rms difference is comparable to that of Willoughby (1990b), who found a value of about 1.4 m s^{-1}. The small average and rms difference confirm the near balance of the hurricane vortex and also provide confidence in the accuracy of the analyzed Doppler winds.

b. Spatially filtered balance

Since Gloria's balanced 500-mb height is unrealistically low, the hydrostatically implied temperature in the layer between 500 mb and the surface is anomalously cold. In order to quantify the anomaly, implied layer-mean temperatures are derived at the vortex center using balanced heights determined at each of the mandatory levels from 100 to 1000 mb. As shown in Fig. 6, the computed layer temperatures below 500 mb are substantially colder than those observed. Much of this anomaly is likely attributable to wind errors inside the eye, where data are nearly absent (cf. Fig. 4).

As also seen in Fig. 6, the lapse rate derived from the balanced heights at the center of Gloria is unstable at 250 mb. The lapse rate can be expressed in terms of the static stability,

$$N^2 \equiv -g\frac{\partial \theta_v}{\partial p} = \frac{g\kappa\Pi}{p}\frac{\partial^2 \phi}{\partial \Pi^2},$$

where p is pressure, g is the gravitational acceleration, $\kappa = R/c_p$ with R being the gas constant and c_p the specific heat for dry air at constant pressure, and $\Pi = c_p(p/p_0)^\kappa$ is the Exner function with p_0 the reference pres-

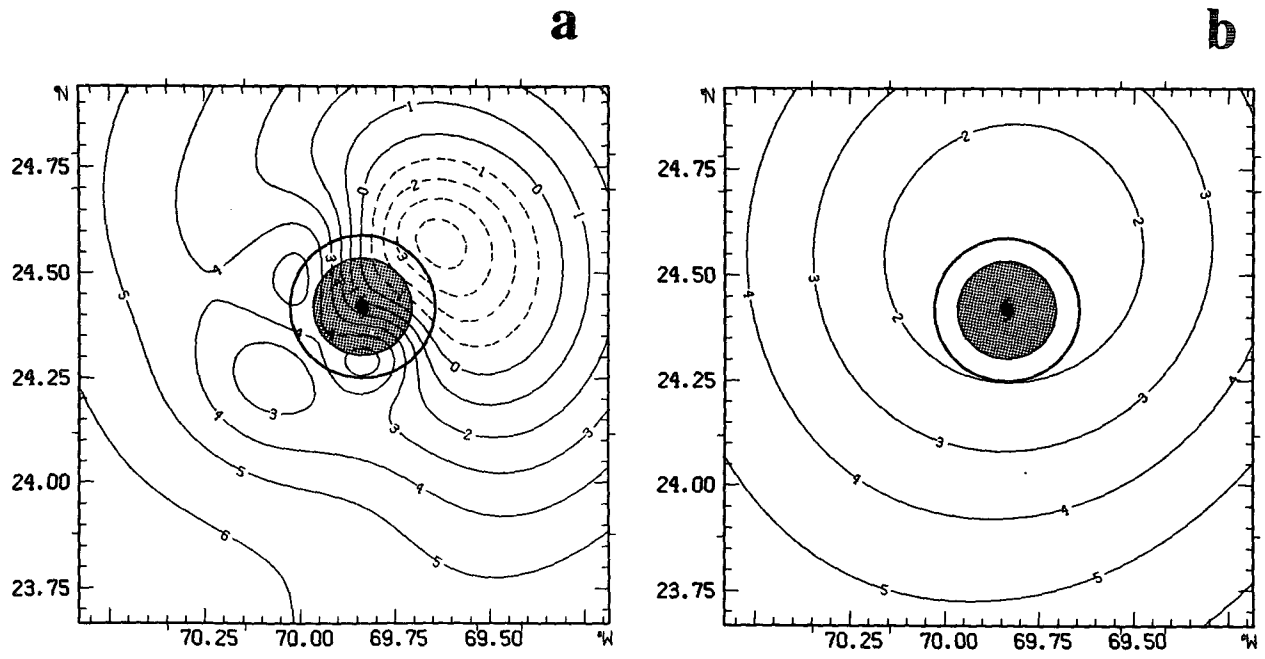

FIG. 7. Static stability at 300 mb for Doppler region (meshes 1–3) from (a) balanced heights and (b) balanced heights from 25-km-scale analyses. Contour interval is 1 × 10^{-3} m^2 K kg^{-1}. Stippling and circle are the same as those in Fig. 2.

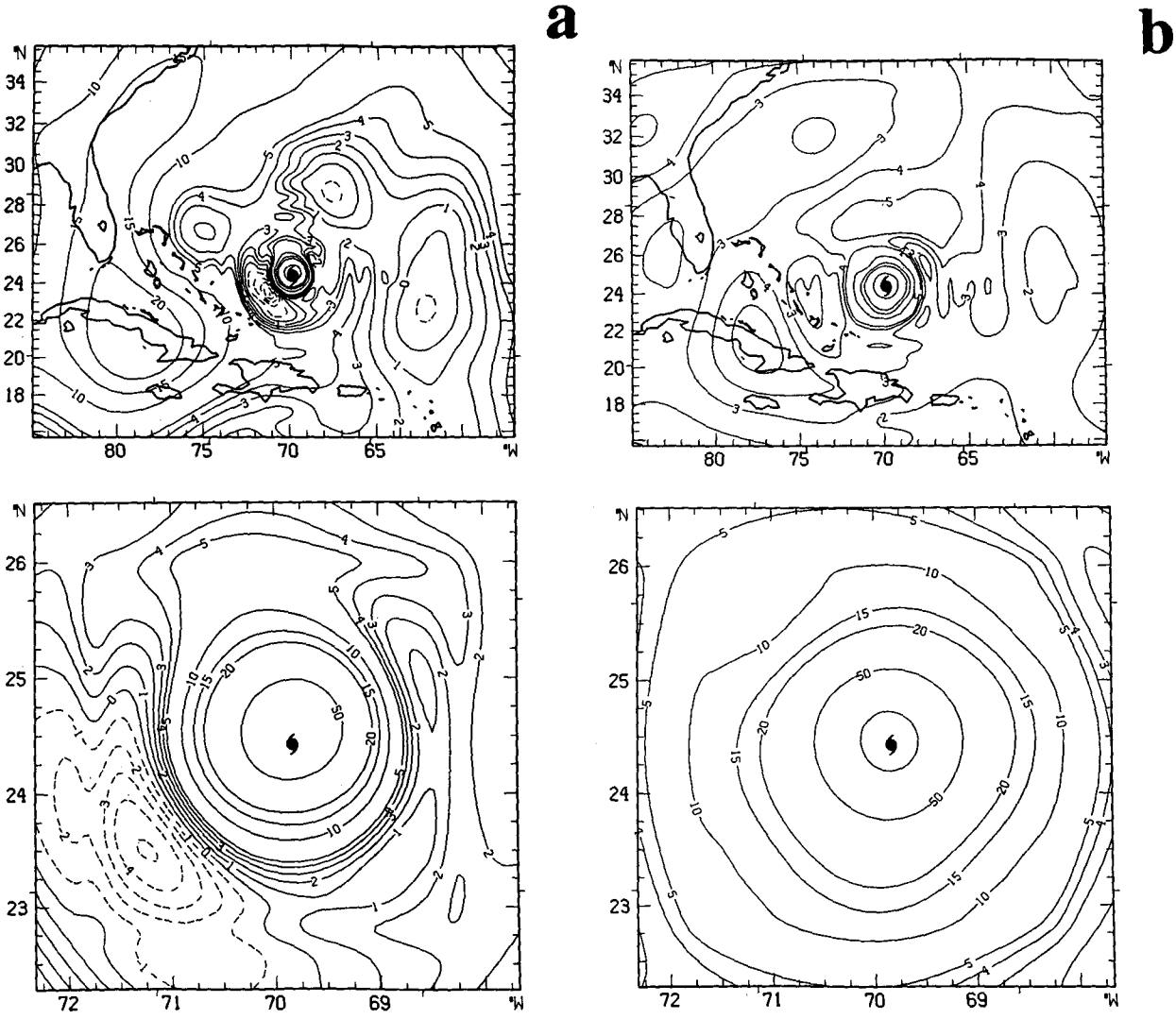

FIG. 8. Potential vorticity from synoptic-scale (meshes 6–7; top) and 25-km-scale (meshes 4–5; bottom) analyses on (a) 350-K (nominally 200 mb), (b) 325-K (nominally 500 mb), and (c) 310-K (nominally 850 mb) surfaces. Contours are 0, ±1, ±2, ±3, ±4, ±5, 10, 15, 20, 50, 100×10^{-7} m^2 s^{-1} K kg^{-1}.

sure of 1000 mb. Vertical derivatives are evaluated from centered finite differences. Figure 7a displays the static stability at 300 mb. Even though the lapse rate is weakly stable ($N^2 > 0$) at the vortex center, there is a strong eyewall-scale (~20 km) asymmetry, including a statically unstable region ($N^2 < 0$) in the northeast quadrant. This unstable region is clearly incompatible with a balanced vortex.

The diagnosed instability is likely due primarily to data deficiencies at the upper levels (see the appendix). Filtering to remove features with the smallest spatial scales will tend to smooth the fields, reduce the influence of data deficiencies, and isolate the balanced part of the phenomenon. Some smoothing in the vertical is already implicit in the use of layer temperatures based on height analyses only at the mandatory levels. As progressively stronger horizontal filters are applied to the Hurricane Gloria analyses, eyewall-scale features are eliminated. In practice, stronger filtering of the winds is accomplished simply by sampling the analyses from successively larger meshes. Application of a filter with wavelength 155.5 km (meshes 5 and higher; see Table 2 of FLFM and the appendix) eliminates the unstable region completely (Fig. 7b). This filter effectively removes features with scales smaller than $155.5/2\pi \approx 25$ km. While the temperatures at the center of Gloria based on the 25-km-scale analyses are still too cold in the lower troposphere (Fig. 6), the lapse rates are relatively close to those observed. Although positive static stability is not itself a sufficient condition for the filtered winds to be in balance, we can conclude that the 25-km-scale filter is both necessary and suffi-

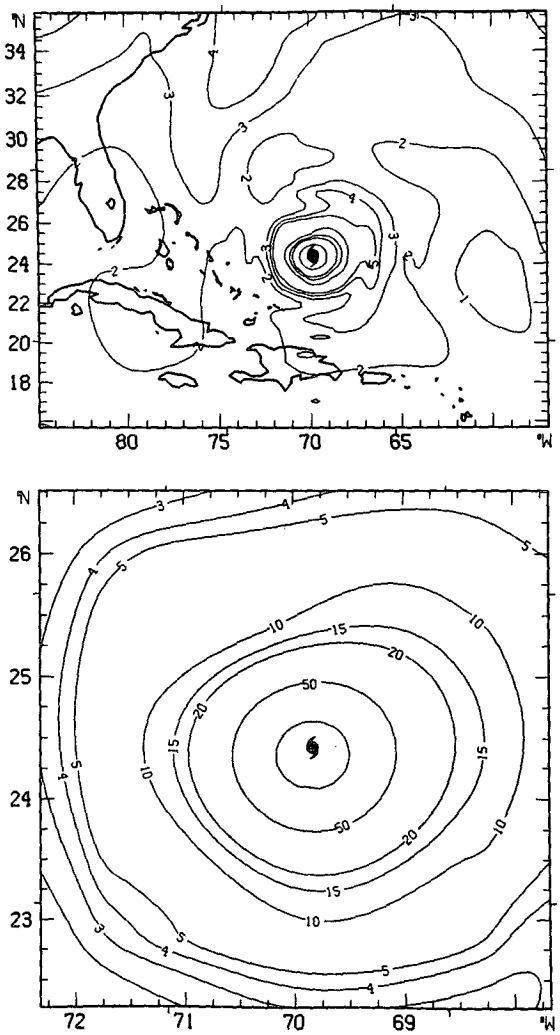

FIG. 8. (*Continued*)

cient to produce geopotential heights that are compatible with a balanced vortex.

3. PV structure

a. 25-km-scale PV

In the process of reducing the influence of data deficiencies, the enhanced filter of section 2b substantially smooths the balanced components of motion in the vortex core. In particular, it reduces the maximum azimuthally averaged tangential wind at 700 mb from 58 to 35 m s^{-1} and moves the RMW outward from 19 to 92 km from the center. The PV structure of the balanced representation of Hurricane Gloria, as derived from the 25-km-scale analyses of section 2b, is shown in Fig. 8. Here PV, denoted q, is defined by

$$q \equiv \frac{g\kappa\Pi}{p}\left[(f+\zeta)\frac{\partial^2\phi}{\partial\Pi^2} - \frac{\partial v}{\partial\Pi}\frac{\partial^2\phi}{\partial x\partial\Pi} + \frac{\partial u}{\partial\Pi}\frac{\partial^2\phi}{\partial y\partial\Pi}\right]$$

[cf. Eq. (2.3) of Davis and Emanuel 1991]. Isentropic analyses were derived by interpolating PV evaluated at the mandatory pressure levels to constant potential temperature surfaces. The 350-, 325-, and 310-K surfaces are near the 200-, 500-, and 850-mb levels, respectively.

The 350-K surface (Fig. 8a) has a region of weakly negative PV to the southwest of the high-PV vortex core, as well as regions of slightly negative PV approximately 500 km to the northeast and 800 km to the east. The resemblance of this PV distribution to the upper-layer PV for a simulated hurricane vortex in

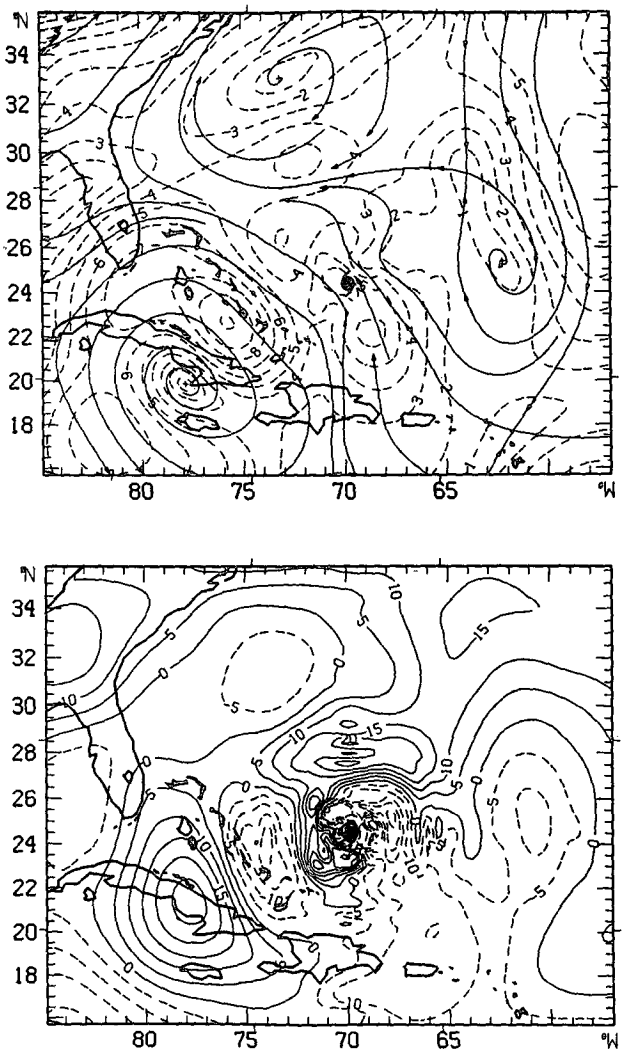

FIG. 9. Asymmetric (top) wind (m s^{-1}, streamlines and isotachs) and (bottom) potential vorticity (contours 0, ±5, ±10, ±15, ±20, ±25, ±50, ±100 × 10^{-8} m^2 s^{-1} K kg^{-1}) from synoptic-scale analyses (meshes 6–7) on the 325-K (nominally 500 mb) surface.

westerly shear shown in Fig. 14 of Shapiro (1992) is striking. In the three-layer isentropic model simulations of Shapiro (1992), a region of negative PV in the upper detrainment layer was generated by twisting terms associated with horizontal gradients of the parameterized cumulus mass flux. Although this region satisfied the necessary condition for local inertial instability, the model simulations did not evidence unstable growth. A region of low PV to the east of the model hurricane was produced inside the vortex core by diabatic heating and then advected by the upper-level westerly wind. A similar evolution has also been described by Wu and Emanuel (1993). The processes that created the negative and low-PV regions in the westerly shear of Shapiro (1992) may also have been operating in Gloria, where the environmental shear was southwesterly (FLFM). An additional feature on the 350-K surface is the positive PV anomaly over Cuba, which is associated with an upper-level cold low. Such positive PV is associated with a cyclonic circulation extending both horizontally and vertically away from the anomaly (Hoskins et al. 1985). This circulation likely had a role in the translation of Hurricane Gloria toward the northwest at this time.

At 325 K (Fig. 8b) the PV is positive everywhere in the region. While the strength of the PV core at the center of the hurricane is about the same as that at 350 K, the magnitude of the PV anomaly over Cuba is smaller. By 310 K (Fig. 8c) the PV anomaly over Cuba has nearly disappeared. About 900 km to the east of the vortex there is a relative PV minimum at both 310 and 325 K, which is approximately coincident with a negative PV anomaly at 350 K. The anticyclonic circulation associated with these negative PV anomalies (Hoskins et al. 1985) may have contributed to Gloria's northwest motion as well.

In order to extract the PV and circulation anomalies that contribute to Gloria's motion, asymmetric fields can be evaluated. The asymmetries (denoted below by primes) are derived by first azimuthally averaging the respective fields on a constant pressure surface about the vortex center. These symmetric averages (denoted by overbars) are then subtracted from the total fields, with the differences then interpolated to an isentropic surface. Large-scale asymmetric wind and PV fields at 325 K are shown in Fig. 9. The asymmetric wind $\mathbf{u}'$ evidences a broad flow across the vortex, which tends to advect the hurricane toward the northwest. The flow lies between opposing gyres. The cyclonic gyre to the southwest of the hurricane is nearly coincident with positive q' over Cuba, while the anticyclonic gyre is nearly coincident with negative q'. As noted above, these PV anomalies are vertically coherent over some depth. In fact, the distribution of q' is very similar to that of vertically averaged asymmetric absolute vorticity on the same spatial scale (Fig. 16 of FLFM). The gyres at 325 K are associated with PV asymmetries above and below, as well as at, that level. Thus one cannot simply infer an association between the wind and PV asymmetries at the single level.

b. *Eyewall-scale PV*

Although the 25-km-scale analyses provide a good representation of the broad PV structure of Gloria and its relationship with the environment, resolution of inner-core eyewall-scale PV requires analyses with the filter characteristics used by FLFM, which are summarized in the appendix. Since three-dimensional in situ thermodynamic measurements are not available, an eyewall-scale PV analysis requires the use of balanced heights derived from these high-resolution analyses to determine the thermodynamic characteristics in the inner region. The 325-K (midtropospheric) distribution of eyewall-scale PV in the inner core of Gloria, based on these balanced heights, is shown in Fig. 10. The vortex forms a plug of PV with radius of about 25 km. Inside this radius the PV asymmetry about the wind center is primarily due to horizontal variations in the balanced temperature and static stability. The amplitude of the predominantly wavenumber 1 asymmetry is about one-half that of the symmetric component. A region of very small negative PV to the southwest of the center is associated with slightly negative absolute vorticity (cf. Fig. 2b).

The 500-mb static stability derived from an ODW sounding in the Doppler region, 60 km to the west of the eye, is within 25% of the 400–700-mb layer stability derived from the balanced heights at the same location. Thus, the PV distribution in Fig. 10, derived

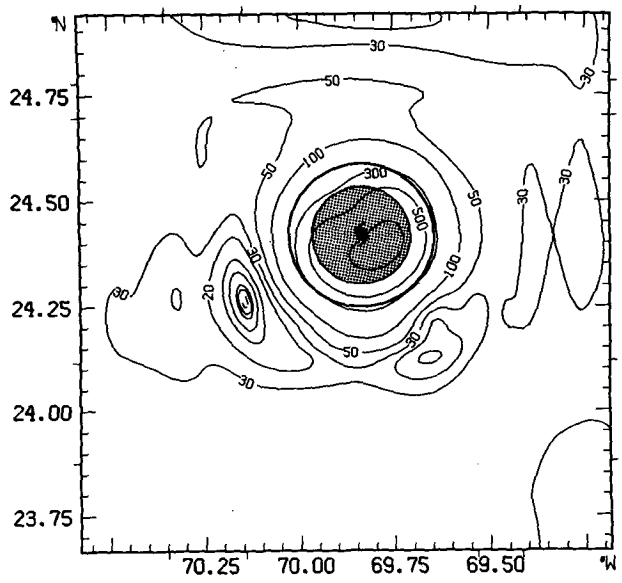

FIG. 10. Potential vorticity from eyewall-scale analyses for Doppler region (meshes 1–3) on the 325-K (nominally 500 mb) surface. Contours are 0, ±1, 5, 10, 20, 30, 50, 100, 300, 500, 1000 × 10^{-7} m^2 s^{-1} K kg^{-1}. Stippling and circle are the same as those in Fig. 2.

for an isentropic surface close to 500 mb, should be relatively realistic. As discussed in section 2b, however, the use of balanced heights derived from analyses that retain eyewall-scale features is in general problematic. Data deficiencies outside the Doppler region, as well as inside the eye, lead to some unrealistic temperatures and static stabilities, particularly at the highest and lowest levels.

The most obvious problems can be avoided by evaluating the eyewall-scale PV associated with the symmetric part of the balanced vortex based on winds restricted to levels from 200 through 850 mb. The symmetric PV is defined by

$$\bar{q} \equiv \frac{g\kappa\Pi}{p}\left[(f_0 + \bar{\zeta})\frac{\partial^2\bar{\phi}}{\partial\Pi^2} - \frac{\partial\bar{V}}{\partial\Pi}\frac{\partial^2\bar{\phi}}{\partial r\partial\Pi}\right],$$

where $\bar{V}$ is the azimuthal average of the tangential velocity V, and $\bar{\phi}$ is determined from gradient wind balance. Here the azimuthal averages are taken about a nominal center determined from flight-level data, and the environmental value of $\bar{\phi}$ at each level is specified at radius $r = 1200$ km. Vertical derivatives at 200 and 850 mb are evaluated from one-sided differences, and static stabilities at these levels are taken from the adjacent levels in the interior of the domain.

The symmetric PV, shown in the radial–height cross section of Fig. 11, is positive everywhere for $r > 13$ km. Extreme values of PV lie inside the RMW. Much weaker local PV maxima occur at $r \sim 100$ km and $r \sim 375$ km, the former associated with a secondary wind maximum noted by Willoughby (1990a). Each of the local PV maxima is associated with a sign reversal in the radial PV gradient on an isentropic surface. In the context of the slow-manifold asymmetric balance formulation of Shapiro and Montgomery (1993), it can be demonstrated that the vortex then satisfies the *necessary* condition for instability of asymmetric disturbances (Montgomery and Shapiro 1995). The stability criterion is strictly valid only for a dry vortex and may possibly be modified in the presence of moisture. Convective heating, including that associated with the hurricane eyewall, tends to create local regions of anomalous PV. Guinn and Schubert (1993b) recently proposed that barotropic instability of an annular region of relatively high PV near the center of a hurricane could result in a polygonal eyewall. Due to the lack of Doppler wind data inside the eye, $\bar{q}$ cannot be reliably estimated inside $r \approx 13$ km. A separate analysis of 450-mb vorticity in the inner core, however, including in situ flight-level data, evidences a local maximum at $r \approx 12$ km. This local maximum implies a positive radial PV gradient, and thus a sign reversal, inside the RMW.

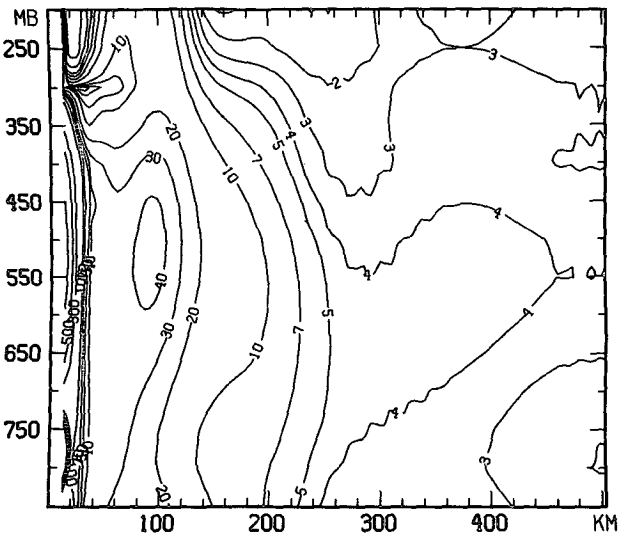

FIG. 11. Radial–height cross section of symmetric PV. Contours are 2, 3, 4, 5, 7, 10, 20, 30, 40, 50, 70, 100, 300, 500, 1000 × 10^{-7} m^2 s^{-1} K kg^{-1}. Values in data-sparse region, within 13 km of vortex center, are not displayed.

4. Summary and discussion

Conservation and invertability properties of PV have been used to considerable advantage in understanding tropical cyclone dynamics. Until now PV analyses have been based on either numerical model results or synoptic-scale analyses (see section 1). The observations in Hurricane Gloria provide the opportunity to resolve features on smaller spatial scales in the inner core and embed analyses of these features within the larger-scale environment.

Due to the absence of three-dimensional thermodynamic measurements in the inner core, balanced geopotential heights were used to derive the PV distributions in section 3. Most of the error in the 500-mb balanced height (section 2a; Fig. 4) within the core but outside the eye was due to errors in the data-sparse region between the Doppler data in the core and the synoptic-scale environment covered by ODWs (see the appendix). Data deficiencies are particularly severe in the upper troposphere above flight level. Smoothing of the wind data using a filter with a minimum 25-km spatial scale was required to derive a geopotential height distribution that was consistent with a statically stable balanced vortex (section 2b). The data deficiencies could be substantially reduced by in situ measurements in the upper troposphere.

Azimuthally averaged 500-mb winds in the core, outside the RMW, were found to be close to gradient balance (section 2a). Due to limited aircraft data, the azimuthal averages were based on only the four cardinal points. The small diagnosed wind imbalance, which occurred in radial bands approximately 10 km wide, could be due to asymmetries that are aliased into the average or to observational uncertainty or error. The analyses also allow two possible physical causes for the imbalance. One possibility is that gradient imbal-

ance is sustained by eddy momentum fluxes associated with convective-scale motions, as proposed by Gray (1962, 1967). These fluxes would have to be much greater than those in the present analyses, however, since an additional analysis of the 500-mb heights (not shown) with the neglected divergence-associated terms (including vertical velocity but excluding the local time tendency) added to (1) produced substantially the same gradient imbalance as that from (1) alone. An alternate possibility is that part of the imbalance is associated with an inertia–gravity oscillation of the symmetric circulation. Since such an oscillation is associated with local radial accelerations, the tangential wind will be out of balance.

The large-scale PV distribution (section 3a) evidences asymmetries in the middle and upper troposphere that appear to be associated with Gloria's translation to the northwest. As noted in section 3a, however, due to the vertical coherence of the PV anomalies one cannot directly infer an association between the wind and PV asymmetries at any single level. In order to associate given PV and wind distributions directly, a piecewise PV inversion, such as that applied by Davis and Emanuel (1991) and expanded upon by Davis (1992), is required. In a separate study, the 25-km-scale PV analyses will be used in the context of a piecewise inversion to extract information on the PV asymmetries at each level that contributed to Gloria's translation.

Acknowledgments. This research was supported in part by the Office of Naval Research Grant N00014-94-F-0045. The authors thank Drs. John Gamache and Hugh Willoughby for reviewing an earlier version of the paper. Dr. Willoughby's insights on many aspects of gradient balance are particularly appreciated.

APPENDIX

Data, Analysis Algorithm, and Methodology

The analyses presented by Franklin et al. (1993) and utilized in the present study were derived from observations of Hurricane Gloria collected from 1800 UTC 24 September to 0230 UTC 25 September 1985. A two-dimensional nested objective analysis algorithm (DeMaria et al. 1992) was used. The algorithm is an extension of the method described by Lord and Franklin (1987) and is based on the Spectral Application of a Finite Element Representation system developed by Ooyama (1987). Gloria's core was sampled by Doppler radar data from 200 to 900 mb. The surrounding environmental flow was primarily sampled by ODWs from 400 to 950 mb, rawinsondes at all levels, PIREPs from 200 to 550 mb, and ships at the surface. Satellite-derived winds were available at 200–400, 500, 850, and 900 mb. Because of the asynoptic nature of the observations, all data were positioned in a storm-relative coordinate system centered at 0000 UTC 25 September. Background wind data were obtained from the global operational spectral analyses of the NOAA National Meteorological Center (NMC) for 0000 UTC. Wind analyses were derived at 50-mb intervals from 100 to 950 mb, as well as at the surface.

Horizontal analyses for each level were generated using identical mesh and filtering parameters, as specified in Table 2 of Franklin et al. (1993). The mesh sizes range from approximately 60 km × 65 km for the innermost mesh 1 to 20 300 km × 10 300 km for the outermost mesh 9. The domains were designed so that the Doppler observations were contained within mesh 3 and the ODWs were contained within mesh 7. Filter wavelengths for each mesh were chosen to be consistent with observation-sampling density wherever possible. Fields of vertical pressure velocity ω were determined for each mesh by integrating the continuity equation upward, where the divergences were corrected so as to satisfy the condition $\omega = 0$ at 100 mb. Since the radar does not see much into the boundary layer, where divergences are large, the vertical velocities will tend to be underestimated.

Important limitations of the analyses were noted by Franklin et al. (1993). The winds in the vortex core were derived using a pseudo-dual-Doppler approach (Jorgensen et al. 1983), with a single aircraft measuring both horizontal wind components. Due to the time separation between measurements of the two components, this method could be expected to reveal only the coarser mesoscale motions with timescales of 45–60 min or more. This approach was probably sufficient for identifying the mean flow in the eyewall and wavenumber 1 asymmetries. Higher-order asymmetries and convective-scale motions, however, may not have been adequately resolved. Other limitations are attributable to the distribution of available observations and the choice of mesh filter wavelength. The uppermost well-sampled level is 200 mb. Reliable synoptic-scale information is confined generally to the region within 1000 km of Gloria's center and over North and Central America. Outside of this area, the analyses closely follow the NMC background fields. Since the environmental analysis between 200 and 450 mb is determined largely by interpolation, the vertical variation of wind in this layer is uncertain. Due to the near absence of Doppler targets inside the eye, reliable analyses in the vortex core are restricted to areas outside the 13-km radius. Inside that radius the analyses are based essentially on extrapolation. An abrupt reduction in data density immediately outside the vortex core required that meshes 1–3 be filtered somewhat more than necessary from data considerations alone and that buffer, or transition, meshes (4 and 5) be inserted between the core and the synoptic environment. The transition meshes are underfiltered, and as a result, the analyses on these meshes have a somewhat noisy appearance.

REFERENCES

Barnes, S. L., 1964: A technique for maximizing details in numerical weather map analysis. *J. Appl. Meteor.*, **3,** 396–409.

Davis, C., 1992: Piecewise potential vorticity inversion. *J. Atmos. Sci.*, **49,** 1397–1411.

——, and K. A. Emanuel, 1991: Potential vorticity diagnostics of cyclogenesis. *Mon. Wea. Rev.*, **119,** 1929–1953.

Demaria, M., S. D. Aberson, K. V. Ooyama, and S. J. Lord, 1992: A nested spectral model for hurricane track forecasting. *Mon. Wea. Rev.*, **120,** 1628–1643.

Fankhauser, J. C., 1974: The derivation of consistent fields of wind and geopotential height from mesoscale rawinsonde data. *J. Appl. Meteor.*, **13,** 637–646.

Franklin, J. L., S. J. Lord, and F. D. Marks, Jr., 1988: Dropwindsonde and radar observations of the eye of Hurricane Gloria. *Mon. Wea. Rev.*, **116,** 1237–1244.

——, ——, S. E. Feuer, and F. D. Marks, Jr., 1993: The kinematic structure of Hurricane Gloria (1985) determined from nested analyses of dropwindsonde and Doppler radar data. *Mon. Wea. Rev.*, **121,** 2433–2451.

Gray, W. M., 1962: On the balance of forces and radial accelerations in hurricanes. *Quart. J. Roy. Meteor. Soc.*, **88,** 430–458.

——, 1967: The mutual variation of wind, shear, and baroclinicity in the cumulus convective atmosphere of the hurricane. *Mon. Wea. Rev.*, **95,** 55–73.

——, 1991: Comments on "Gradient Balance in Tropical Cyclones." *J. Atmos. Sci.*, **48,** 1201–1208.

Guinn, T. A., and W. H. Schubert, 1993a: Hurricane spiral bands. *J. Atmos. Sci.*, **50,** 3380–3403.

——, and ——, 1993b: Polygonal eyewalls in hurricanes. Preprints, *20th Conf. on Hurricanes and Tropical Meteorology,* San Antonio, TX, Amer. Meteor. Soc., J30–J31.

Haltiner, G. J., and R. T. Williams, 1980: *Numerical Prediction and Dynamic Meteorology.* 2d ed., Wiley, 477 pp.

Hoskins, B. J., M. E. McIntyre, and A. W. Robertson, 1985: On the use and significance of isentropic potential vorticity maps. *Quart. J. Roy. Meteor. Soc.*, **111,** 877–946.

Jorgensen, D. P., P. H. Hildebrand, and C. L. Fousch, 1983: Feasibility test of an airborne pulse-Doppler meteorological radar. *J. Climate Appl. Meteor.*, **22,** 744–757.

Lord, S. J., and J. L. Franklin, 1987: The environment of Hurricane Debby (1982). Part I: Winds. *Mon. Wea. Rev.*, **115,** 2760–2780.

Montgomery, M. T., and Shapiro, L. J., 1995: Generalized Charney–Stern and Fjortoft theorems for rapidly rotating vortices. *J. Atmos. Sci.*, in press.

Ooyama, K. V., 1987: Scale controlled objective analysis. *Mon. Wea. Rev.*, **115,** 2479–2506.

Schubert, W. H., and B. T. Alworth, 1987: Evolution of potential vorticity in tropical cyclones. *Quart. J. Roy. Meteor. Soc.*, **113,** 147–162.

Shapiro, L. J., 1992: Hurricane vortex motion and evolution in a three-layer model. *J. Atmos. Sci.*, **49,** 140–153.

——, and M. T. Montgomery, 1993: A three-dimensional balance theory for rapidly rotating vortices. *J. Atmos. Sci.*, **50,** 3322–3335.

Thorpe, A. J., 1985: Diagnosis of balanced vortex structure using potential vorticity. *J. Atmos. Sci.*, **42,** 397–406.

Willoughby, H. E., 1990a: Temporal changes of the primary circulation in tropical cyclones. *J. Atmos. Sci.*, **47,** 242–264.

——, 1990b: Gradient balance in tropical cyclones. *J. Atmos. Sci.*, **47,** 265–274.

——, 1991: Reply. *J. Atmos. Sci.*, **48,** 1209–1212.

Wu, C.-C., and K. A. Emanuel, 1993: Interaction of a baroclinic vortex with background shear: Application to hurricane movement. *J. Atmos. Sci.*, **50,** 62–76.

——, and ——, 1995: Potential vorticity diagnostics of hurricane movement. Part I: A case study of Hurricane Bob (1991). *Mon. Wea. Rev.*, **123,** 69–92.